

A geometric view of formation control with application to directed sensing*

Louis Theran * Daniel Zelazo ** Jessica Sidman ***

* School of Mathematics and Statistics, University of St Andrews, Scotland (e-mail: lst6@st-andrews.ac.uk).

** Stephen B. Klein Faculty of Aerospace Engineering, Technion - Israel Institute of Technology, Haifa, Israel (e-mail: dzelazo@technion.ac.il)

*** Department of Mathematics, Amherst College, Amherst, MA, USA (e-mail: jsidman@amherst.edu)

Abstract: We propose a geometric approach to distance-based formation control modeled on a minimum-norm lifting of Riemannian gradient descent in edge-space to node-space. This yields a unified family of controllers, including the classical gradient controller and its directed variant. For the directed case, we give a simple numerical test for local convergence that applies to any directed graph and target. We show that persistence is neither necessary nor sufficient for local convergence of our directed controller and propose an alternative that is necessary and more easily checked.

Keywords: formation control; nonlinear control; multi-agent systems; rigidity theory

1. INTRODUCTION

The distance-constrained formation control problem has emerged as one of the canonical problems for multi-agent coordination. The objective is to steer a group of agents to a prescribed geometric shape, specified by inter-agent distances, using only local sensing and distributed control actions. The classical solution, by Krick et al. (2009), is a gradient-based controller that uses the squared edge length error as a potential in node space and follows the negative gradient. When the sensing graph is generically d -rigid, the gradient controller is generically locally exponentially stable, as shown by Sun et al. (2016), using tools from rigidity theory. In a notable work, Dörfler and Francis (2010) introduced a differential-geometric perspective to the problem that indicates the squared edge lengths evolve on a manifold of feasible distances in edge space.

A more realistic model of the problem is the *directed* variant, in which each distance constraint is assigned to one agent. The resulting interactions become non-reciprocal and lose their potential-gradient structure. As a result, directed formation control is significantly less well-understood. Much of the existing literature focuses on specific graph families derived from *persistence*, which is a property of a directed graph that attempts to adapt rigidity theory to the directed setting motivated by the role of d -rigidity in the solution to the undirected problem (Krick et al. (2009) and Theorem 2); see also Hendrickx et al. (2007); Anderson et al. (2007); Yu et al. (2009); Babazadeh and Selmic (2020). A complementary line of

work by Zhang et al. (2018) introduces gain design to recover stability with directed sensing; they are able to do this for the highly restricted class of persistent graphs in leader / first-follower form.

In this work, we take a different perspective on the directed problem. Instead of working with a property of oriented graphs, we work with d -rigid graphs and impose a condition on the quadratic form derived from a modification of the rigidity matrix that incorporates the data of the graph orientation (Theorem 3). This connects the information from the directed graph to the manifold of feasible distance measurements, a core object of study in rigidity theory. It also allows us to identify open, semialgebraic regions of the target space on which the dynamics are local exponentially stable, and to provide combinatorial certificates when no such region exists (Theorem 4). Summarizing, we initiate a new, structural theory of robust directed formation control.

The approach to the directed formation control problem described above rests on taking a differential-geometric viewpoint of the distance-based formation control focused on the dynamics of an artificial edge-space system evolving on the manifold of feasible measurements. Riemannian gradient descent on the edge manifold, followed by a minimum norm lift to node dynamics gives a geometrically canonical “model” solution to formation control (Section 2). While not practically useful in a distributed setting, the model controller serves as a template for a family of controllers that includes the model, gradient, and directed controllers (Section 3). We derive a simple condition, that can be checked with linear algebra, for local exponential stability in this family (Theorem 1) that implies generic exponential convergence of the model and gradient controllers (Theorem 2). Then we specialize to the directed

* This work was supported by the Israel Science Foundation grant no. 453/24 and UK Research and Innovation though the grant UKRI1112. We thank the ICMS in Edinburgh, where this project was initiated, for its hospitality.

controller, giving a simple, numerical condition sufficient for local exponential convergence that applies to any graph and target formation (Theorem 3). Simulations in Section 5 validate our theory and illustrate that local exponential stability is not a generic property of the directed controller, showing that persistence is neither necessary nor sufficient in the directed setting. This leads us to introduce the notions of dynamic and algebraic admissibility, which are generic properties of a directed graph that can be easily checked, and which we prove to be necessary for local exponential stability of the directed controller (Theorem 4) in Section 6.

Notations: We write \mathbb{R} for the set of real numbers and \mathbb{Q} for the set of rational numbers. For a matrix A , we write A^\top for its transpose and A^\dagger for its Moore–Penrose pseudoinverse. We use $A \succ 0$ ($A \succeq 0$) to indicate that A is symmetric positive definite (semidefinite). The image, kernel, and rank of A are written $\text{Im } A$, $\text{Ker } A$, and $\text{rk } A$. For a subspace W , its orthogonal complement is W^\perp . For a smooth map F , the differential at x is denoted dF_x . All inner products are Euclidean unless stated otherwise, and $\|\cdot\|$ denotes the associated norm for vectors, and induced norm for operators. For a manifold \mathcal{M} , $T_x\mathcal{M}$ denotes its tangent space at x and $\text{grad}_{\mathcal{M}}V$ denotes the Riemannian gradient of a smooth function $V: \mathcal{M} \rightarrow \mathbb{R}$. The quadratic form of an operator T is denoted $q_T(x) := \langle x, T(x) \rangle$, and the restriction of T to a subspace V is denoted $T|_V$.

2. THE FORMATION CONTROL PROBLEM

In this section, we briefly review the standard formulation of the formation control problem and then introduce a closely related, artificial problem that exposes its underlying geometric structure.

The starting point for this work is with an ensemble of n agents, modeled by integrator dynamics,

$$\dot{p}_i(t) = u_i(t), \quad i = 1, \dots, n, \quad (1)$$

where $p_i(t) \in \mathbb{R}^d$ is the state (position) of agent i , and $u_i(t) \in \mathbb{R}^d$ is the control. The aggregate position (control) vector is denoted as $p(t) = [p_1(t)^\top \cdots p_n(t)^\top]^\top$ (similarly for $u(t)$). We assume the agents interact by an information exchange network described by the undirected graph $\mathcal{G} = (\mathcal{V}, \mathcal{E})$.

The *target configuration* p^* has an associated set of desired inter-agent square distances, m_{ij}^* , for each $ij \in \mathcal{E}$; $m^* \in \mathbb{R}^{|\mathcal{E}|}$ is the aggregate target distance vector. We define the *distance map* $F: \mathbb{R}^{dn} \rightarrow \mathbb{R}^{|\mathcal{E}|}$ by

$$F(p) = [\cdots \|p_j - p_i\|^2 \cdots]^\top, \quad (2)$$

so that $F(p^*) = m^*$. From now on, the squared edge length measurement of a target formation p^* will be denoted m^* . The distance-based formation control problem is to drive an initial configuration p^0 to a point q congruent and close to p^* (such that $F(q) = m^*$), using, at each time t , the information m^* and $m(t) = F(p(t))$. We introduce two assumptions that we will use at various points in this paper.

Assumption 1. The graph \mathcal{G} is generically d -rigid and the target configuration p^* is a regular point of the rigidity map F .

Assumption 2. The graph \mathcal{G} is generically d -rigid and the target configuration p^* is generic.

Here generic means that p^* holds over the open, dense complement of an unspecified exceptional set that is defined by polynomials with rational coefficients. Every generic configuration is regular, and if p^* is generic, then $F(p^*)$ is generic in the image of F . A graph \mathcal{G} is d -rigid if, for every configuration p^* so that $F(p^*)$ is smooth in the image of F , the framework (\mathcal{G}, p^*) is locally rigid; in particular, when \mathcal{G} is d -rigid, the frameworks (\mathcal{G}, p^*) for regular p^* will be rigid (Gortler et al. (2010)).

2.1 The Standard Control Law

In the standard formulation of the formation control problem, a common approach is to use a negative-gradient flow of the potential function $V(p) = \frac{1}{4}\|F(p) - m^*\|^2$, yielding the control

$$u(t) = -\frac{\partial V(p(t))}{\partial p(t)} = -R(p(t))^\top(R(p(t))p(t) - m^*). \quad (3)$$

Here, we note that $R(p(t))p(t) = F(p(t))$, where $R(p(t)) \in \mathbb{R}^{nd \times |\mathcal{E}|}$ is known as the *rigidity matrix*. This control ensures local exponential convergence to a configuration q near p^* such that $F(q) = m^*$, which, if \mathcal{G} is d -rigid will imply that q is congruent to p^* (see, e.g., Krick et al. (2009); Sun et al. (2016); Dörfler and Francis (2010) and Theorem 2).

2.2 The Edge System

The work of Dörfler and Francis (2010) analyzed (3) from a geometric perspective. The starting point of that analysis was to consider the dynamics of distances, i.e., $\frac{d}{dt}F(p(t))$. In this work we take a similar approach, although our starting point will not be the agent level dynamics defined by (3). Rather, we will assume the existence of an artificial system of edges with state $m(t) \in \mathbb{R}^{|\mathcal{E}|}$ that evolve according to the integrator dynamics

$$\dot{m}(t) = v(t), \quad (4)$$

for some control $v(t)$. In the “edge space” we now seek a control to drive the edge states to the desired set of square distances m^* .

We emphasize that, unless $n \leq d + 1$, there must be algebraic constraints on $v(t)$ to ensure that $m(t)$ evolves in a way that is consistent with a physical system; i.e., that there is a $p(t)$ such that $F(p(t)) = m(t)$ for all t . Since the constraint is that $m(t)$ lies in the image of F , we denote by \mathcal{Q} the regular values of the map F . Because F is a polynomial mapping defined over \mathbb{Q} , the semialgebraic Sard theorem (Bochnak et al., 1998, p. 234) implies that \mathcal{Q} is a smooth semialgebraic set that is open and dense in the image of F . (The image of F itself is not smooth. We will see presently why we use \mathcal{Q} instead of the smooth locus of $\text{Im } F$.) We also note that $\mathcal{C} := F^{-1}(\mathcal{Q}) \subseteq \mathbb{R}^{dn}$, the set of regular points of F , is a smooth semi-algebraic set of dimension dn . At any point $m = F(p)$ in \mathcal{Q} , the tangent space $T_m\mathcal{Q}$ is the vector space of differential changes to the squared edge lengths that can arise from the infinitesimal motions of the agents, i.e.,

$$T_m\mathcal{Q} = \text{Im } R(p).$$

Accordingly, the edge dynamics (4) are to be interpreted as evolving on \mathcal{Q} , meaning that the velocity $v(t)$ must satisfy $v(t) \in T_{m(t)}\mathcal{Q}$ for all t .

The manifold \mathcal{Q} inherits the Euclidean inner product from $\mathbb{R}^{|\mathcal{E}|}$, defining a Riemannian metric,

$$g_m(\xi_1, \xi_2) = \xi_1^\top \xi_2, \quad \xi_1, \xi_2 \in T_m \mathcal{Q}.$$

Let $\Pi(m) : \mathbb{R}^{|\mathcal{E}|} \rightarrow T_m \mathcal{Q}$ denote the orthogonal projector onto $T_m \mathcal{Q}$. If m is a regular value of F , for any $p \in F^{-1}(m)$, we have

$$\Pi(m) = R(p)R^\dagger(p). \quad (5)$$

(Note that if m is smooth but not regular, then the formula for $\Pi(m)$ will be valid for some p in the fiber over m but not others.)

Define the *edge potential* function,

$$V_e(m) = \frac{1}{2}\|m - m^*\|^2,$$

which measures the squared deviation of the current edge vector m from the desired one m^* . As we are interested in feasible motions that must remain on \mathcal{Q} , the appropriate notion of the gradient is the *Riemannian gradient* on (\mathcal{Q}, g) , obtained by projecting $\nabla V_e(m) = m - m^*$ onto the tangent space of \mathcal{Q} at m ,

$$\nabla_{\mathcal{Q}} V_e(m) = \Pi(m) \nabla V(m) = \Pi(m) (m - m^*).$$

The *Riemannian gradient flow* associated with V_e is defined by

$$\dot{m} = -\nabla_{\mathcal{Q}} V_e(m) = -\Pi(m) (m - m^*). \quad (6)$$

A solution to (6) describes a trajectory $m(t) \in \mathcal{Q}$ whose velocity $\dot{m}(t)$ is the projection of the negative Euclidean gradient of V_e onto the tangent space $T_{m(t)}\mathcal{Q}$. Hence, the motion remains on \mathcal{Q} for all time and follows the steepest descent of V_e with respect to the Riemannian metric g .

2.3 Connecting Edge Flows to Node Flows

To connect the squared edge length flow defined by the Riemannian gradient flow in (6) to node dynamics, we make use of the fact that $\mathcal{Q} = F(\mathcal{C})$. At any configuration $p \in \mathcal{C}$, the differential of the edge map F is the map

$$dF_p : T_p \mathcal{C} \longrightarrow T_{F(p)} \mathcal{Q},$$

where we recall that $dF_p = 2R(p)$. This linear map relates infinitesimal changes of the node positions $\dot{p} = u$ to infinitesimal changes of the squared edge lengths via

$$\dot{m} = dF_p u = 2R(p) u.$$

Hence, to produce a prescribed edge-space velocity $v^* \in T_{F(p)}\mathcal{Q}$, we seek a node-space velocity u satisfying

$$dF_p u = v^*.$$

Among the infinitely many u that satisfy this relation, a natural choice is the one with *minimum Euclidean norm*:

$$\min_{u \in \mathbb{R}^{dn}} \|u\|^2 \quad \text{s.t.} \quad dF_p u = v^*. \quad (7)$$

The unique minimizer of (7) is obtained via the Moore-Penrose pseudoinverse,

$$u^* = (dF_p)^\dagger v^* = 2R(p)^\dagger v^*.$$

This solution corresponds to the *minimum-norm configuration velocity* that generates the desired edge-space motion v^* .

The mapping dF_p^\dagger provides the least-energy lift of an admissible edge velocity to a consistent motion of the agent configuration. Consequently, the combined edge-node system can be viewed as a two-level geometric control construction:

- (1) In edge space, compute the Riemannian gradient flow $v^* = -\nabla_{\mathcal{Q}} V_e(m)$, which defines the optimal tangent velocity on \mathcal{Q} .
- (2) In node space, realize this motion through the minimum-norm lift $u^* = dF_p^\dagger v^*$.

Substituting $v^* = -\Pi(m)(m - m^*)$ yields the node-space dynamics

$$\dot{p} = u^* = -\frac{1}{2} R(p)^\dagger \Pi(m) (m - m^*). \quad (8)$$

This expression represents the *minimum-energy configuration flow* that is consistent with the Riemannian steepest-descent dynamics on the edge manifold.

We refer to (8) together with (6) as the *model controller*. This control, while not distributed as in (3), provides a clear geometric picture of what should be done to drive agents to a desired formation.

3. FROM THE MODEL CONTROLLER TO DISTRIBUTED SOLUTIONS

While the model controller (6) and (8) represents a geometrically canonical approach to solving the formation control problem, it is not intended as an algorithm for practical implementation. Instead, we use it as a template for a new design space of controllers with the same essential characteristics: edge dynamics evolving on \mathcal{Q} and lifted node dynamics. The larger class is big enough to include distributed architectures such as (3) and controlled enough to be amenable to combinatorial analysis.

3.1 Edge-driven controller family

Now we introduce the control family we study in this section. The state space for the controllers is

$$\mathcal{S} = \{(p, m) \in \mathcal{C} \times \mathcal{Q} : F(p) = m\},$$

which is a smooth, irreducible, semi-algebraic set equipped with the natural projections π_1 and π_2 . At any point $(p, m) \in \mathcal{S}$, its tangent space is

$$T_{(p,m)} \mathcal{S} = \{(\dot{p}, \dot{m}) : \dot{m} = 2R(p)\dot{p}\},$$

which is the same coupling of node and edge velocities that we have seen in the derivation of the model law (8) and (6). We will study control laws determined by state-dependent linear transformations

$$\nu_{(p,m)} : \mathbb{R}^{|\mathcal{E}|} \rightarrow (\mathbb{R}^d)^n \quad \text{and} \quad \eta_{(p,m)} : \mathbb{R}^{|\mathcal{E}|} \rightarrow \mathbb{R}^{|\mathcal{E}|},$$

such that $(\nu_{(p,m)}x, \eta_{(p,m)}x) \in T_{(p,m)} \mathcal{S}$ for all states in \mathcal{S} and vectors $x \in \mathbb{R}^{|\mathcal{E}|}$. Given a target formation (\mathcal{G}, p^*) with edge measurements m^* and a starting formation (\mathcal{G}, p^0) , the controller is the initial value problem (IVP)

$$\dot{p} = \nu_{(p,m)}(m^* - m) \quad (9a)$$

$$\dot{m} = \eta_{(p,m)}(m^* - m) \quad (9b)$$

with initial conditions

$$\begin{cases} \dot{p}(0) &= \nu_{(p^0, F(p^0))}(m^* - F(p^0)) \\ \dot{m}(0) &= \eta_{(p^0, F(p^0))}(m^* - F(p^0)). \end{cases}$$

For technical reasons, we will also allow controllers to be defined only on an open neighborhood in \mathcal{S} of (p^*, m^*) .

Controllers in this family yield solutions $(p(t), m(t)) \in \mathcal{S}$. When we discuss the *edge dynamics* of one of these controllers, we mean the flow $\pi_2(p(t), m(t)) \in \mathcal{Q}$, and the node dynamics are, similarly, $\pi_1(p(t), m(t)) \in \mathcal{C}$. The edge and node dynamics have the same smoothness as the full solution. For notational ease, we use the shorthand $\eta := \eta_{(p,m)}$ and $\eta^* := \eta_{(p^*,m^*)}$ (similarly for ν). In the following examples we illustrate how the model and gradient controllers fit into this setup. With an eye to applying algebraic geometry, we show that the transformations $\eta_{(p,m)}$ and $\nu_{(p,m)}$ are rational functions of the state.

Example 1. (Model controller, revisited). The model controller (6) and (8) arises from setting

$$\nu = \frac{1}{2}R^\dagger(p) \quad \text{and} \quad \eta = \Pi(m) = 2R(p)\nu.$$

The formulas for η and ν contain the pseudo-inverse of $R(p)$, which is analytic in the state, but not rational. However, in a neighborhood of p^* , we can define the projectors as rational functions if we fix the indices of the columns of a basis for the column space of $R(p)$. Thus, there is a neighborhood of (p^*, m^*) on which the model law is defined by rational functions. \diamond

Example 2. (Gradient controller, revisited). The classical gradient law arises from setting

$$\nu = R^\top(p) \quad \text{and} \quad \eta = 2R(p)R^\top(p).$$

These are polynomial functions of the state (p, m) , which are rational over all of \mathcal{S} . The column space of η is contained in the column space of $R(p)$, and, hence, in $T_m\mathcal{Q}$. By construction, we have $2R(p)\nu = \eta$, so the controller is well-defined. \diamond

We note that the matrix η in Example 2 is not a projection, since it does not fix its image pointwise.

3.2 Local exponential stability

We now provide a sufficient condition for the local exponential stability of (9) to a generic target.

Theorem 1. (Local exponential stability). Let Assumption 1 hold. Suppose that for some neighborhood $V \subseteq \mathcal{S}$ of (p^*, m^*) , the linear transformations ν and η are rational functions of $(p, m) \in V$. If the quadratic form q_{η^*} restricted to $T_{m^*}\mathcal{Q}$, is positive definite, then there is a neighborhood $U \ni (p^*, m^*)$ such that the control law determined by (9a)–(9b) with initial condition $(p^0, F(p^0)) \in U$ converges to a state (q, m^*) with q congruent to p^* . Moreover, the edge dynamics on \mathcal{Q} and the node dynamics on \mathcal{C} are locally exponentially stable. \diamond

We remark that, in the proof of Theorem 1, given in Sec. 3.3, the assumption that the controller is rational can be substantially relaxed, to, e.g., C^2 . With rationality, we get, additionally, the algebro-geometric notion of genericity, which corresponds to structural robustness of the control law. The local exponential convergence certificate given by the positivity of q_{η^*} will, if it holds at one point, hold on an open semialgebraic subset of target configurations. Hence, non-robust stability is *non-generic*, and the sufficient condition provided in Theorem 1 is robust to perturbation in the target geometry. For the model and gradient controllers, the situation is even better, and local

convergence is a generic property. Although the sufficient stability condition in Theorem 1 is strictly stronger than the linearized dynamics being Hurwitz, for these two controllers, it is also necessary, yielding an extremely clean, combinatorial theory.

Theorem 2. (Generic undirected exponential stability). Let Assumption 1 hold. Then there exists a neighborhood U of p^* such that the node dynamics on \mathcal{C} of the model controller (8), (6), and the gradient controller (3) onto \mathcal{C} converge exponentially to a configuration congruent to p^* for any initial condition $p \in U$ if and only if \mathcal{G} is d -rigid. \triangle

Proof. The case where \mathcal{G} is not d -rigid is easier, so we do it first. If \mathcal{G} is not d -rigid, because p^* generic, every neighborhood of p^* contains a configuration q not congruent to p^* such that $F(p^*) = F(q)$. At this q , both the model and gradient controllers will immediately stop (i.e., $\dot{p} = 0$). Hence, they do not locally converge to a configuration congruent to p^* .

Now suppose that \mathcal{G} is d -rigid. The semialgebraic Sard Theorem (Bochnak et al., 1998, p. 234) implies that p^* is a regular point of F , so $(p^*, m^*) \in \mathcal{S}$, putting us in the general setting of Theorem 1, which we use to show local exponential convergence. Examples 1 and 2 show that the model and gradient controllers are rationally defined and satisfy the other hypotheses of Theorem 1. What remains is to check that q_{η^*} is positive definite. In both laws, the $\eta_{(p,m)}$ matrix is PSD with columns spanning $T_m\mathcal{Q}$. Since the restriction of a PSD matrix to its column space is positive definite, the result follows. The verification of PSD in the model controller is because $\Pi(m)$ is a projector and in the gradient controller because $\eta = 2R(p)R(p)^\top$ is presented as factoring. \square

The conclusion for the gradient controller is due to Krick et al. (2009) and has been reproved many times in the literature.

3.3 Proof of Theorem 1

Let us fix a target $(p^*, m^*) \in \mathcal{S}$. The goal is to find a neighborhood $U \subseteq \mathcal{S}$ of (p^*, m^*) so that there are:

- (I) Constants $C, c > 0$ such that, for all initial conditions $(p^0, m^0) \in U$, and all $t \geq 0$, $\|m^* - m(t)\| \leq Ce^{-ct}$;
- (II) Constants $K, k > 0$ such that, for all initial conditions $(p^0, m^0) \in U$, there is a configuration q congruent to p^* , such that $\|q - p(t)\| \leq Ke^{-kt}$.

The proof is geometric and illustrates many of the ideas leading to the derivation of the model controller and larger family. Along the way, we mention connections to standard techniques in control theory and rigidity.

Node stability from edge stability We first assume that (I) holds and derive (II). The essence of the argument is that smoothness of ν implies that the edge-to-node dynamics are input-to-state stable (ISS). Rigidity enters here because, locally, the fiber $F^{-1}(m^*)$ consists of configurations congruent to p^* . Now we give the formal argument.

Assume (I), i.e., there are constants $C, c > 0$ and a neighborhood $V \subseteq \mathcal{Q}$ of m^* so that, for all initial conditions $(p^0, m^0) \in F^{-1}(V) \times V$, $\|m^* - m(t)\| \leq Ce^{-ct}$.

Because \mathcal{G} is d -rigid and p^* is a regular value of F , we can find a neighborhood U_0 of p^* so that if $q \in U$ and $F(q) = m^*$, then q is congruent to p . Let us now consider the full dynamics in the neighborhood $U = (U_0 \cap F^{-1}(V)) \times V$ of the target (p^*, m^*) . Shrinking U , if necessary, we can find an $N > 0$ so that $\|\nu\| < N$, because ν is rational in the state, and so its eigenvalues remain bounded on a neighborhood of (p^*, m^*) . Using our estimate on $\|\nu\|$, we obtain

$$\|\dot{p}(t)\| = \|\nu(m^* - m)\| \leq N\|m^* - m\| \leq \underbrace{NC}_{C'} e^{-ct}.$$

Consider a sequence $t_i \rightarrow \infty$, and let $j > i$. We have

$$\|p(t_j) - p(t_i)\| \leq \int_{t_i}^{t_j} \|\dot{p}(t)\| dt \leq \int_{t_i}^{\infty} C' e^{-ct} dt \leq \frac{C'}{c} e^{-ct_i}.$$

Hence, the sequence $p(t_i)$ is Cauchy, and has a limit q . A similar estimate give us

$$\|q - p(t)\| \leq \frac{C'}{c} e^{-ct},$$

so the convergence is exponential. Since the whole state converges to $(q, m^*) \in \mathcal{S}$, we have $F(q) = m^*$ and $q \in U_0$, so q is congruent to p^* . This completes the proof of (II) assuming (I). We remark that, had we not assumed exponential convergence, some additional effort would be required to show the node dynamics do not become trapped in the space of rigid motions.

Exponential stability in edge space This is the core technical argument, and it proceeds parallel to a standard line in Lyapunov stability theory. The key novelty is that, using the geometric perspective, we identify a geometrically canonical quadratic energy, namely q_{η^*} on $T_{m^*}\mathcal{Q}$, that certifies local exponential convergence in a way that can be verified computationally.

The proof of (I) will follow once we have a neighborhood $V \subseteq \mathcal{Q}$ of m^* so that, for $m \in V$ we have the coercive inequality

$$q_{\eta}(m^* - m) \geq \alpha\|m^* - m\|^2, \quad (10)$$

for some $\alpha > 0$. Using (10), we get

$$\frac{d}{dt}\|m^* - m(t)\|^2 = -2q_{\eta}(m^* - m) \leq -2\alpha\|m^* - m\|^2,$$

from which a standard application of Grönwall's inequality (Khalil, 2002, Lemma A.1) yields exponential convergence of any solution of the edge dynamics with initial condition in V . The same estimate shows that $(p, m) \mapsto (\nu, \eta)$ is a smooth vector field on $F^{-1}(V) \times V$, so the solution exists, and the statement for edge convergence holds. Hence, we have (I), up to the construction of V .

By compactness and the hypothesis that η^* induces a positive definite quadratic form on $T_{m^*}\mathcal{Q}$, there is a $\beta > 0$ so that $q_{\eta^*}(x) > \beta$ for all unit vectors x in $T_{m^*}\mathcal{Q}$.

For each $m \neq m^*$, we write $e = \frac{m^* - m}{\|m^* - m\|}$ and then $e = v + w$, where $v \in T_{m^*}\mathcal{Q}$ and $w \in (T_{m^*}\mathcal{Q})^\perp$. Because \mathcal{Q} is an embedded smooth manifold, for all $\varepsilon > 0$ there is an $r > 0$ so that, when $\|m^* - m\| < r$, $\|v\| \geq 1 - \varepsilon$ and $\|w\| < \varepsilon$. After repeated applications of this fact and smoothness of

η in the state, we find a neighborhood V of m^* on which for all $m \in V$ and $(p, m) \in F^{-1}(V) \times V$,

$$\|v\| > 1/2 \quad (11)$$

$$\|w\| < \beta/(32\|\eta^*\|) \quad (12)$$

$$\|w\|^2 < \beta/(16\|\eta^*\|) \quad (13)$$

$$\|\eta^* - \eta\| < \beta/16. \quad (14)$$

This is possible because the constants on the right are independent of m and smoothness of η in the state. We claim this V works. We first lower bound, for $m \in V$,

$$q_{\eta^*}(m^* - m) = \|m^* - m\|^2 q_{\eta^*}(e).$$

From the decomposition of e , we have

$$q_{\eta^*}(e) = q_{\eta^*}(v) + w^\top \eta^* v + v^\top \eta^* w + q_{\eta^*}(w).$$

From the (11),

$$q_{\eta^*}(v) > \beta/4.$$

From (12) and $\|v\| \leq \|e\| = 1$, we get

$$|w^\top \eta^* v| + |v^\top \eta^* w| \leq 2\|v\|\|w\|\|\eta^*\| < \beta/16$$

and, using (13)

$$q_{\eta^*}(w) \leq \|w\|^2 \|\eta^*\| < \beta/16.$$

Combining these bounds yields

$$q_{\eta^*}(e) \geq \beta/4 - 2\beta/16 = \beta/8.$$

Hence, for $m \in V$,

$$q_{\eta^*}(m^* - m) \geq (\beta/8)\|m^* - m\|^2.$$

Finally, by (14),

$$q_{\eta}(e) \geq (\beta/8 - \|\eta^* - \eta\|)\|e\|^2 \geq \beta/16\|m^* - m\|^2,$$

which proves (10) with $\alpha = \beta/16$. This completes the proof of (II). \square

4. DIRECTED CONTROL LAWS

An appealing feature of the gradient control (3) is that it admits a *distributed* implementation. At the agent level, (3) is equivalent to

$$u_i = \sum_{ij \in \mathcal{E}} (\|p_i - p_j\|^2 - m^*)(p_j - p_i). \quad (15)$$

Each agent therefore only requires information from its neighboring agents defined by the graph \mathcal{G} . The model controller (8), however, leads to a *centralized* architecture, since the pseudo-inverse of the rigidity matrix will generally be dense.

While distributed architectures are advantageous, even the control (15) has shortcomings. Indeed, the control assumes bidirectional information exchange. In many real-world applications, it is more realistic (especially with on-board sensing) that the information exchange should be *directed*, i.e., agent i sensing agent j does not imply agent j is sensing agent i . We model this asymmetry by orienting the edges of the sensing graph \mathcal{G} . Given an orientation $\overrightarrow{\mathcal{G}}$ on the edges of \mathcal{G} , we may simply modify (15), as in Zhang et al. (2018), to

$$u_i = \sum_{\substack{i \rightarrow j \\ \in \mathcal{E}}} (\|p_i - p_j\|^2 - m^*)(p_j - p_i), \quad (16)$$

where $\overrightarrow{i,j}$ is the directed edge from node i to j . This leads to the aggregate dynamics, which is no longer a gradient flow, of

$$\dot{p} = -\overrightarrow{R}(p(t))^\top (R(p(t))p(t) - m^*), \quad (17)$$

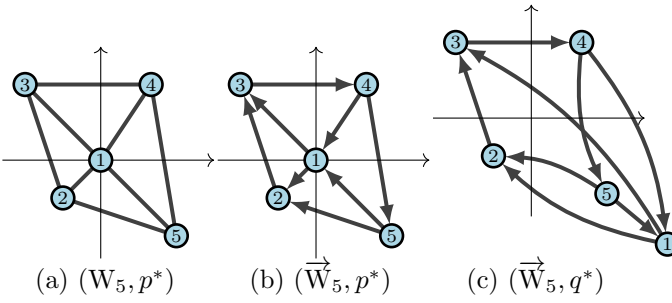


Fig. 1. (a) and (b) have the same target configuration; (b) and (c) have the same orientation, but p^* satisfies Theorem 3 while q^* does not.

where $\vec{R}(p)$ is obtained from $R(p)$ by zeroing out, in the row corresponding to ij , the entries corresponding to the node j for the orientation \overrightarrow{ij} and the entries corresponding to i for the orientation \overleftarrow{ij} . We now describe a numerical test that is sufficient for (17) to converge to a given configuration (\mathcal{G}, p^*) . Since it is based on Theorem 1, this result inherits the same structural stability properties.

Theorem 3. (Exponential stability of (17)). Let Assumption 1 hold, and $(p^*, m^*) \in \mathcal{S}$ be the target state. Let $\vec{\mathcal{G}}$ be an orientation of \mathcal{G} . Let P be a matrix with linearly independent columns spanning the column space of $R(p^*)$ and $Z = 2R(p)\vec{R}(p)^\top$. If $\frac{1}{2}P^\top(Z + Z^\top)P$ is positive definite, then then trajectories of (17) starting sufficiently close to p^* converge exponentially to a configuration q with $F(q) = m^*$. \triangle

Proof. The edge dynamics for the directed law (17) are given by

$$\dot{m} = 2R(p) \left[-\vec{R}(p)^\top(m - m^*) \right].$$

So, in the setting of Theorem 1, the directed control law corresponds to setting

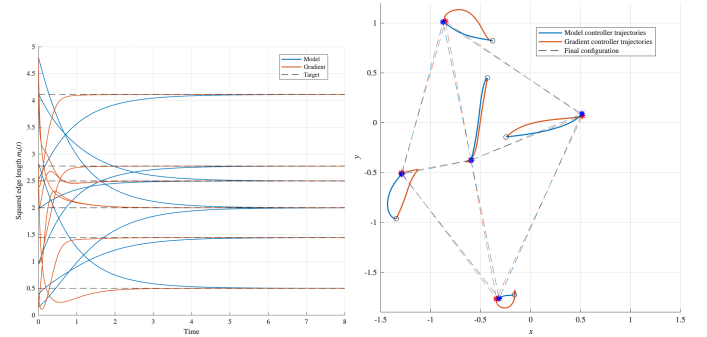
$$\nu := \vec{R}(p)^\top, \text{ and } \eta := 2R(p)\vec{R}(p)^\top = Z.$$

The stated convergence result is an application of Theorem 1, so we check the hypotheses. That \mathcal{G} is generically d -rigid has been assumed, as has $(p^*, m^*) \in \mathcal{S}$. The symmetric matrix $\frac{1}{2}P^\top(Z + Z^\top)P$ corresponds to the quadratic form of η^* restricted to $T_{m^*}\mathcal{Q}$, so, when it is positive definite Theorem 1 applies, and we conclude the convergence result. \square

Even though the directed controller does not have a gradient-potential structure, the stability certificate in Theorem 3 is a natural geometric counterpart to the gradient potential for the directed setting.

5. NUMERICAL STUDIES

We illustrate the behavior of the model controller (8), the gradient controller (3), and the directed controller (17) on representative examples.



(a) Squared edge length trajectories under the model controller (blue) and gradient controller (red). (b) Node trajectories and final configurations for both controllers.

Fig. 2. We compare the model controller (8) and gradient controller (3) for (W_5, p^*) .

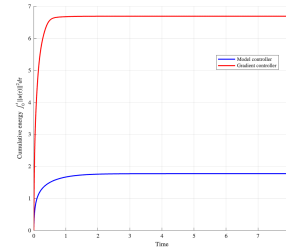
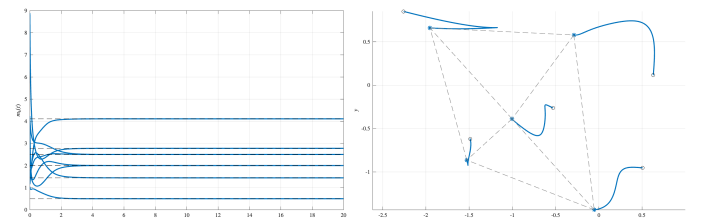


Fig. 3. Cumulative control energy for the model controller (blue) and gradient controller (red) for (W_5, p^*) .

Comparison of the model and gradient controllers We begin with the wheel graph W_5 with node 5 as hub (Figure 1(a)). Figure 2 compares the model controller (8) with the gradient controller (3). Both achieve the desired distances (Figure 2a), but the model controller requires significantly less control energy (Figure 3), as predicted by (7). The resulting trajectories differ, but in both cases the formation converges to a configuration congruent to p^* (Figure 2b).

Target dependence of directed control We next consider the directed wheel \vec{W}_5 (Figure 1(b)). For target p^* , the directed controller satisfies the sufficient condition in Theorem 3, and the trajectories in Figure 4 show exponential convergence.

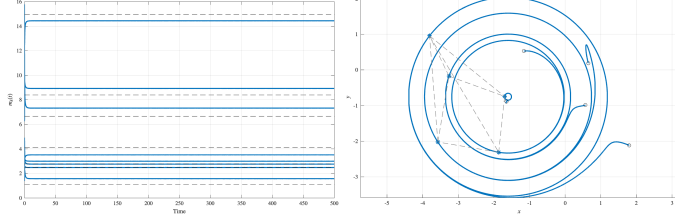


(a) Squared edge length trajectories under the directed controller. (b) Node trajectories and final configuration.

Fig. 4. Trajectories of the directed controller (17) for (\vec{W}_5, p^*) , which satisfies Theorem 3.

In contrast, with the *same orientation* but different target q^* (Figure 1(c)), the numerical test fails and the system

exhibits qualitatively different behavior: the edge lengths converge, but the node trajectories approach a stable limit cycle (Figure 5). Thus, stability depends essentially on *target geometry* and not merely on graph orientation.



(a) Squared edge trajectories under the directed controller.
(b) Node trajectories converge to a limit cycle.

Fig. 5. Trajectories of the directed controller (17) for (\vec{W}_5, q^*) , which does not satisfy Theorem 3.

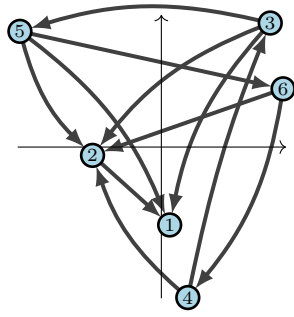
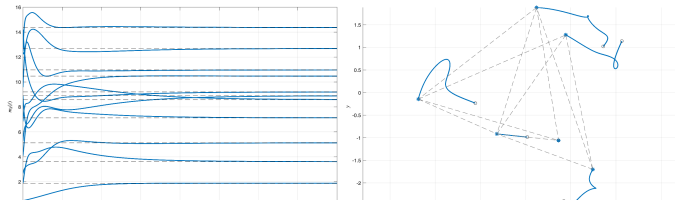


Fig. 6. A directed graph that is not persistent.

Persistence is not necessary Our final example uses the non-persistent directed graph $\vec{\mathcal{G}}$ in Figure 6. Although the directed graph fails the persistence criterion (Hendrickx et al., 2007, Theorem 3), the underlying undirected graph is 2-rigid and the sufficient condition in Theorem 3 is satisfied. As shown in Figure 7, the directed controller again converges.



(a) Squared edge trajectories under the directed controller.
(b) Node trajectories and the final configuration.

Fig. 7. Trajectories of the directed controller (17) for $(\vec{\mathcal{G}}, p^*)$, for a non-persistent graph $\vec{\mathcal{G}}$.

6. AFTER PERSISTENCE: ADMISSIBILITY

We have shown that persistence does not describe the behavior of the directed controller (17). Indeed, Figure 5 shows that it is not sufficient (not sensitive to the target geometry), while Figure 7 shows that persistence is not necessary (not linked to the geometry and dynamics). We now describe an alternative inspired by the algebraic shadow of the dynamics in the family (9).

We begin with the linearized edge dynamics of a controller in the family (9) at a target configuration $(p^*, m^*) \in \mathcal{S}$. Considering a perturbation $(\delta p, \delta m) \in T_{(p^*, m^*)}\mathcal{S}$ and using the notation $e = m^* - m$ for the edge vector, we get $\dot{e} = -\delta m$, so $\dot{e} = -\eta^* \delta m$. Hence, the linearized edge dynamics on $T_{m^*}\mathcal{Q}$ are described by the linear ODE

$$\dot{e} = -\eta^*|_{T_{m^*}\mathcal{Q}} e. \quad (18)$$

From the linear dynamics at the target we define two generic properties of such a controller.

Definition 1. A controller (9) defined by rational functions is called *dynamically admissible* if, for every generic target configuration $(p^*, m^*) \in \mathcal{S}$, $\eta^*|_{T_{m^*}\mathcal{Q}}$ is hyperbolic. It is called *algebraically admissible* if $\eta^*|_{T_{m^*}\mathcal{Q}}$ is invertible for generic targets.

Dynamic admissibility (all eigenvalues have non-zero real parts) implies algebraic admissibility (no eigenvalue is zero). Admissibility is our proposed replacement for persistence when studying the directed controller (17). Both types of admissibility are easy to check with a randomized algorithm: pick a random configuration p^* and then check the eigenvalues of $\eta_{(p^*, F(p^*))}$. Admissibility can be checked independently of the target because it concerns generic eigenstructure, as opposed to the certificates in Theorems 1 and 3, which are about Lyapunov geometry near the target. We also note that the test for both types of admissibility is polynomial time, while the test for persistence described by Hendrickx et al. (2007) is exponential in the number of redundant edges, and, when $d \geq 3$, also uses linear algebra.

We finish by connecting admissibility to the convergence properties of our controllers.

Theorem 4. (Admissibility is necessary). Let Assumption 2 hold. If a controller defined by (9a)–(9b) defined by rational functions is locally exponentially stable for some target formation $(p^*, m^*) \in \mathcal{S}$, then it is dynamically admissible. \triangle

Proof. By Corollary 4.3 in Khalil (2002) (used in an appropriate chart on \mathcal{Q}), if a non-linear IVP converges exponentially, the linearization of the dynamics at the equilibrium must be Hurwitz, and, hence hyperbolic. From (18), this implies that $\eta^*|_{T_{m^*}\mathcal{Q}}$ is hyperbolic. Because dynamic admissibility is a generic property, one example where it is satisfied implies the result. \square

In particular, dynamic and algebraic admissibility are *necessary* for local exponential convergence of any control law in our family. This is in parallel to the one direction of the role of generic d -rigidity for the model and undirected controllers: a combinatorial constraint that any locally stable design must satisfy.

7. FURTHER DIRECTIONS

Our work suggests some immediate open problems. A combinatorial classification of the dynamically and algebraically admissible orientations of a graph is a natural next step, and it would be interesting to identify special families of d -rigid graphs and orientations for which the sufficient condition in Theorem 3 holds generically. It would also be of interest to know whether the sufficient

stability condition in Theorem 3 is also necessary, as it is in Theorem 2.

ACKNOWLEDGEMENTS

We thank Ashley Bao, Martin Deraas, Shlomo Gortler, Karime Hernandez, Tony Nixon, Bernd Schulze and Audrey St John for helpful conversations and feedback.

REFERENCES

- Anderson, B.D., Dasgupta, S., and Yu, C. (2007). Control of directed formations with a leader-first follower structure. In *46th IEEE Conference on Decision and Control*, 2882–2887.
- Babazadeh, R. and Selmic, R.R. (2020). Distance-based formation control over directed triangulated laman graphs in 2-d space. In *59th IEEE Conference on Decision and Control*, 2786–2792.
- Bochnak, J., Coste, M., and Roy, M.F. (1998). *Real algebraic geometry*. Springer.
- Dörfler, F. and Francis, B. (2010). Geometric analysis of the formation problem for autonomous robots. *IEEE Transactions on Automatic Control*, 55(10), 2379–2384.
- Gortler, S.J., Healy, A.D., and Thurston, D.P. (2010). Characterizing generic global rigidity. *American Journal of Mathematics*, 132(4), 897–939.
- Hendrickx, J.M., Anderson, B.D.O., Delvenne, J.C., and Blondel, V.D. (2007). Directed graphs for the analysis of rigidity and persistence in autonomous agent systems. *International Journal of Robust and Nonlinear Control*, 17(10-11), 960–981.
- Khalil, H.K. (2002). *Nonlinear Systems*. Prentice Hall, Upper Saddle River, NJ, 3 edition.
- Krick, L., Broucke, M.E., and Francis, B.A. (2009). Stabilisation of infinitesimally rigid formations of multi-robot networks. *International Journal of Control*, 82(3), 423–439.
- Sun, Z., Mou, S., Anderson, B.D., and Cao, M. (2016). Exponential stability for formation control systems with generalized controllers: A unified approach. *Systems & Control Letters*, 93, 50–57.
- Yu, C., Anderson, B.D.O., Dasgupta, S., and Fidan, B. (2009). Control of minimally persistent formations in the plane. *SIAM Journal on Control and Optimization*, 48(1), 206–233.
- Zhang, P., de Queiroz, M., Khaledyan, M., and Liu, T. (2018). Control of directed formations using interconnected systems stability. *Journal of Dynamic Systems, Measurement, and Control*, 141(4), 041003.